Journal of Materials Chemistry A

Accepted Manuscript

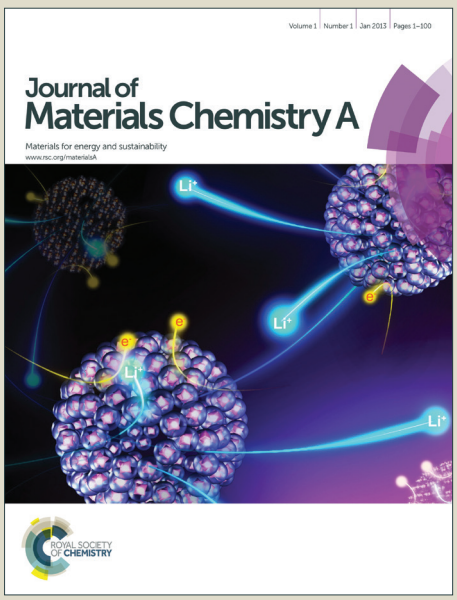

ROYAL SOCIETY OF CHEMISTRY

www.rsc.org/materialsA

Journal Name

RSCPublishing

ARTICLE

Environmentally Benign Magnetic Chitosan/Fe_3O_4 Composites as Reductant and Stabilizer for Anchoring Au NPs and Their Catalytic Reduction of 4–nitrophenol

Cite this: DOI: 10.1039/x0xx00000x

Received 00th January 2012,
Accepted 00th January 2012

DOI: 10.1039/x0xx00000x

www.rsc.org/

Yunfeng Qiu,[a] Zhuo Ma[b] and PingAn Hu*[a],

We report the facile synthesis of environmentally benign Au NPs/chitosan composites and magnetic Au NPs/chitosan/Fe_3O_4 composites without employing any toxic reductants or capping agents. Renewable natural chitosan not only functioned as supporting matrix, but also served as reductant and stabilizer for the formation and dispersions of Au NPs. Fe_3O_4 nanopheres were easily embedded into the chitosan matrix due to the strong complexation ability of chitosan with Fe_3O_4, which originated from the sharing of the lone electron pairs from the nitrogen atom in amine with Fe^{II} or Fe^{III} on the surface of Fe_3O_4. The as–prepared magnetic composites exhibited much higher activities, as well as more convenient magnetic recyclability than other supported Au NPs towards the reduction of 4–nitrophenol. From the practical point of view, apart from good performance of the reduction of nitro compounds, the biocompatibility and biodegradability of present Au NPs/chitosan/Fe_3O_4 composites promote the potential applications in biochemical catalysis or therapy.

Introduction

Noble metal nanoparticles (NPs) have drawn great attention due to their superior chemical and physical properties such as catalysis, optical and electronic properties, as well as biological applications.[1–4] Among reported noble NPs, the study of Au NPs is one of the most active research areas during the past decades because of their unusual physicochemical properties.[5–8] Various shapes and sizes of Au NPs have been subjected to many important applications in bio–sensor, bio–analysis, thermal therapy of cancer, gene delivery, and catalysis, showing high performance.[9–12] Particularly, Au NPs have higher Fermi potential, which leads to the lowering of reduction potential value comparing to bulks, and hence nanosized Au NPs can function as a catalyst for many electron–transfer reactions, such as the reduction of aromatic nitro compounds or dyes.[13, 14]

Generally, Au NPs without any protecting agents are easy to assemble into large aggregates *via* the interparticle dipolar force, resulting in the decrease of specific surface area and the loss of quantum effect, which would impede the application in catalysis.[15, 16] Fortunately, the introduction of capping agents on the surface of Au NPs could solve the aggregation problem, and thus extend the application fields.[17, 18] The preparation methods of stable Au NPs generally utilized laborious solution strategies and toxic reagents, such as organic solvents and excessive capping agents, which is strongly against the basic principle of green chemistry and sustainability of our society. Additionally, in both academic and industrial catalytic fields, the feasible separation and the recycle of catalyst from the reaction mixture were of great importance because of their high cost and environmental hazards.[19–22] Small Au NPs possess better catalytic performance than larger ones, which however make it difficult to separate completely from the catalytic systems due to the stringent filtration and centrifugation requirements. Such conflict can be readily solved by the immobilization of Au NPs on the supports, which has been proved to be an effective way.[23–25] Most inorganic nanosized solid supports such as SiO_2, ZrO_2, TiO_2, QDs, and graphene have attracted much attention due to their large surface areas, strong affinity with Au NPs, and synergetic effects in terms of the combination of individual advantage.[26–29] It is worth mentioning that the multistep synthesis of solid supports and loading procedures of Au NPs make the whole process lengthy and uncertain. And the conventional reduction of Au NPs always utilizes the strong reducing agents to trigger the nanoparticle nucleation and growth, or alkaline metal solutions, which in other words are harmful to the environment.[30]

Alternatively, Au NPs could also be loaded on the matrix of polymers due to their abundant hydroxyl, carboxyl, or pyridine groups, and thus strong coordination effects are existed between them.[24, 31–34] Polymer–Au NPs composites exhibited intriguing properties in the application of sensors, actuators, electrodes for fuel cells, catalysis, and in optical and electronic devices.[31–34] Also, advantages of polymer including mechanical and processible properties, and the optical, electrical and catalytic properties of Au NPs can be suitably integrated to achieve superior performance due to the synergistic effects.[35] However, it is noteworthy that these artificial polymers always need tedious synthetic procedure and multi purification steps

besides the harshness of naturally degradable condition. As the emphasis of science and technology is to shift more towards environmentally friendly and sustainable resources and processes, it is highly appealing to develop renewable and green Au NPs/polymer composites. Therefore, biodegradable and biocompatible biopolymers containing superior coordination sites for anchoring metal ions might be the ideal alternative candidates in replacing the artificial polymer.[34] For example, chitosan, which is the second most abundant natural polymer in the word after cellulose, is considered as a suitable solid biopolymer support for the immobilization of metal catalyst.[36, 37] Additionally, the biocompatibility and antibacterial properties of chitosan and being an eco–friendly polyelectrolyte makes it intriguing for various applications such as water treatment, hybrid fibers for textiles, biomedical devices and drug delivery.[38, 39] Thus it is speculated that Au NPs/chitosan composite would be suitable for various commercial applications, especially if Au NPs are fabricated under green protocols.[40] For instance, Yang et.al. reported that chitosan was a very effective reducing and stabilizing agent for the preparation of Au NPs.[41] Schauer et.al. found that both carboxymethyl chitosan and chitosan could be used to synthesize and stabilize Au NPs in the presence of excessive sodium borohydride as reducing agent.[42] Qu's group studied the degradation of chitosan during the formation of Au NPs in terms of various viscosity of chitosan solution.[43] However, the recovery of Au NPs from nanosized solid supports or biopolymer stabilized hybrid systems are not satisfactory, and thus greatly waste the catalyst and generate metal contaminants, and also make the observing of the reaction progress extremely difficult due to the presence of suspended nanoparticles in reaction solution.

Design magnetic catalytic systems proved to be an effective way to solve the aforementioned issues, since the magnetic separation technique possesses the advantages of rapidity, high efficiency, and cost–effectiveness.[44, 45] Additionally, the magnetic recovery systems will effectively eliminate the requirement for either solvent swelling before or catalyst filtration after the reaction.[46] Obviously, the introduction of magnetic advantage into the Au NPs/chitosan composite has so many benefits, but the related work is seldom reported.[47] Therefore, it is highly appealing to design a green protocol to fabricate Au NPs/chitosan composite, and a facile way to incorporate the magnetic particles into this system to solve the recovery issues and make the most of the function of each individual component.

We hereby present a facile way to prepare Au NPs using chitosan as the reducing and stabilizing agent without any other stronger protecting or reducing agents, such as citrate or $NaBH_4$, and successfully incorporate Fe_3O_4 nanoparticles into the composite. In addition, the catalytic performances of magnetic composite with respect to efficiency and recyclability were also evaluated for the reduction of 4–nitrophenol in the presence of $NaBH_4$.

Experimental

Reagents

Chitosan flakes, from crab shells (Practical grade >85% deacetylated; viscosity < 200 mPa·s) were purchased from Shenyang National Chemical Company. Analytical grade Sodium borohydride ($NaBH_4$), hydrogen tetrachloroaurate hydrate (Hydrochloroauric acid·$3H_2O$), 4–nitrophenol ($C_6H_5NO_3$), $FeCl_3·6H_2O$, anhydrous CH_3COONa, and Ethylene glycol were purchased from Aladdin Industrial Corporation. All compounds were used as received. All solutions were prepared with triply distilled water.

Characterization

UV–vis spectra were recorded in UV–2550. The FT–IR spectra of the prepared catalysts were collected on a Perkin–Elmer 1710 Fourier transform spectrometer by KBr pellet method at room temperature. The XRD patterns were obtained on a Shimadzu 6000 powder diffraction system (40kV, 100mA), using Cu$K\alpha$ radiation (λ= 0.1541 nm) in a scanning range of 2−80° at a scanning rate of 1 °/min. The magnetic properties were collected using vibrating sample magnetometry (VSM) at room temperature. SEM observations were performed on an FEI Quanta 200 scanning electron microscope. The acceleration voltage was set to 10 kV. The sample was stuck on the observation platform and sprayed with platinum vapor under high vacuum for about 90 s. The characterization of Au NPs was performed using a field emission TEM (TecnaiG2F30, FEI, US). 1 mg of sample was sonicated in 1 mL ethanol for 10 min. The ethanol slurry was then dropped onto a Cu grid covered with a thin film of carbon.

Formation of Au NPs/chitosan composites

The synthesis of Au NPs/chitosan composites were performed by mixing chitosan flakes to an aqueous solution of $HAuCl_4·3H_2O$. In a typical procedure, 100 mg of chitosan flakes were added to a round–bottom flask with 10 mL deionized water. The pH value of solution is adjusted to 6.0 ± 0.1 by 1 M HCl and 1 M NaOH aqueous solution. Afterwards, a certain volume of hydrochloroauric acid stock solution was injected. The mixture was stored in dark room for 20 min for the equilibrated absorption of $AuCl_4^{-1}$ by chitosan until the supernatant solution became colorless. The flask was incubated in an oil bath at 50 ^oC for 20 h. The colour of chitosan flakes incorporating $AuCl_4^{-1}$ turned into wine red gradually. The final product was filtered and stored in dark room.

Formation of Au NPs/chitosan/Fe_3O_4 composites

The synthesis of Fe_3O_4 was performed according to previous literatures.[48, 49] In a typical procedure, 0.5 g of $FeCl_3·6H_2O$ was dissolved in 25 mL deionized water. Afterwards, 2 g of CH_3COONa and 2 g of polyethylene glycol were added, followed by stirring for another 10 min. The mixture was then transferred to a stainless steel autoclave and heated under 180 °C for 12 h. The black product was washed with ethanol several times by filtration and was dried at 50 °C in a vacuum oven. The as–synthesized Fe_3O_4 was dispersed into chitosan aqueous solution including 0.05 M acetic acid. The Fe_3O_4/chitosan composite was precipitated by the addition of 1 M NaOH aqueous solution, followed by filtration and washed triply by deionized water. The synthesis of Au NPs on Fe_3O_4/chitosan composite was similar to the procedure of Au NPs/chitosan. The final product was separated by applied magnetic field and stored in dark room.

General procedure for the reduction of 4–NP

In a typical reaction, 1 mL of 0.01 mol·L^{-1} 4–NP was added to 20 mL of 0.01 mol·L^{-1} $NaBH_4$ aqueous solution. Subsequently, 50 mg of 0.3125 wt% composites was added. After addition of Au NPs/chitosan, the characteristic absorption peak of 4–nitrophenolate ion at 400 nm gradually decreased.

Simultaneously, a new peak at ~295 nm, ascribable to newly generated 4–AP, emerged. The absorption spectra of the solution were recorded in the range of 250–550 nm. The rate constants of the reduction process (k_{app}) were determined using the following equations: $-dC_t/dt = kC_t$ and $\ln(C_t/C_0) = -kt$. The reduction reaction of 4–NP with $NaBH_4$ in the absence of composites and in the presence of chitosan have also been carried out under similar condition.

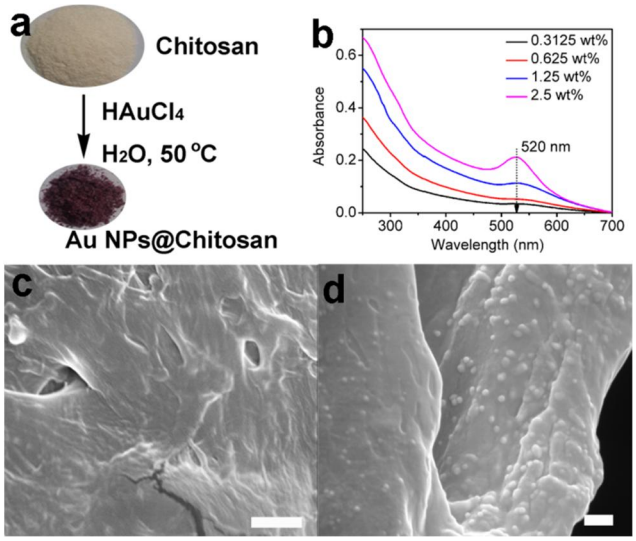

Fig. 1 (a) Digital images of light yellow chitosan powder and wine red Au NPs/chitosan powder. (b) UV–vis spectra of Au NPs/chitosan composite as a function of varying Au loading amounts. The characteristic peaks of Au NPs are centered at ca. 520 nm for all cases. (c) Scanning electronic microscopy (SEM) image of chitosan. (d) SEM image of Au NPs/chitosan composite, in which Au particles were clear to observe on the surface of chitosan. The crack and blurry regions were caused by electron beam damage due to the poor conductivity of chitosan. Scale bars are 1 μm in (c), and 100 nm in (d).

Results and discussion

It is well known that chitosan has been regarded as an absorption material for removing metal ions from waste water because of the strong complexation ability of amine groups with metal ions.[50] Inspired from previous works, the basic procedure for the formation of Au NPs/chitosan composite contains two steps. First, the gold ions were adsorbed onto chitosan.[43] Subsequently, the Au^{n+} species were reduced by hydroxyl groups in chitosan. Based on these pioneering assumptions, it is possible to synthesize Au NPs/chitosan composite under mild conditions without using any additives by reasonable design of synthesis procedure. As shown in **Fig. 1a**, the colour of Au NPs/chitosan powder became wine red after exposure of chitosan flakes to aqueous solution of hydrochloroauric acid under thermal incubation at 50 °C for 20 h. **Fig. 1b** shows the characteristic surface plasmon resonance (SPR) band centered at 520 nm for Au NPs, suggesting the successful synthesis of Au NPs. As shown in **Fig. S2**, the wine red deepens gradually as a function of reaction time, as well as the increasing concentration of hydrochloroauric acid, which is attributed to the increasing content of Au NPs. Moreover, the thermal induced reduction of hydrochloroauric acid can only occur at elevated temperature in an appropriate time. The colour of reaction slurry mixture was unchanged at room temperature after aging for 24h, which indicates the reduction reaction barrier energy can not be effectively overcome at lower temperature. This experimental phenomenon is consistent with previous result, in which the reduction of hydrochloroauric acid by chitosan did not occur even when incubated for 12h at 45 °C.[51] In present case, the elevation of reaction temperature will accelerate the reaction rate greatly, and thus the wine red emerged quickly. Additionally, chitosan is regarded as a reducing and stabilizing agent for the synthesis of metal particles. The samples synthesized in the absence of chitosan, however, were always light yellow belonging to the intrinsic colour of hydrochloroauric acid aqueous solution, which is also confirmed by the silent band centered at 520 nm in the UV–vis region. It is found that the reduction reaction proceeds smoothly at pH 6.0 ± 0.1 due to the favorable hydrolyzation of hydrochloroauric acid salts by hydroxyl radicals, and hence promotes the reduction of hydrochloroauric acid by chitosan. Therefore, the presence of chitosan, suitable pH value and elevated temperature will guarantee the formation of Au NPs.

SEM images in **Fig. 1c** and **1d** show the morphologies of chitosan flakes before and after loading Au NPs. It is clear to observe the Au spheres on the surface of chitosan comparing to the pristine chitosan with moderately smooth surface. A thin layer of platinum was sputtered on the surface to enhance the conductivity. Meanwhile the thickness was thinner than conventional samples for avoiding the coverage of the Au NPs. Therefore, transmission electron microscopy (TEM) measurement was performed to further confirm the formation of Au NPs as illustrated in **Fig. 2**. Obviously, the nanoparticles were formed successfully, and distributed evenly without obvious agglomeration. Meanwhile, there are only slight difference in particle size and size distribution (22 ± 2 nm) under different Au loading. It is noteworthy that higher reaction temperature such as 80 °C could result in aggregates of particles due to the fast nucleation and growth as reported in previous work. Additionally, some triangles and large spheres are mixing with the nanoparticles at 80 °C.[51] Therefore, lowering the reaction temperature to 50 °C will facilitate the growth of Au NPs in a moderately mild condition.

The coordination interaction between Au NPs and chitosan was assessed by FTIR measurements. As shown in **Fig. 3**, FTIR spectra of chitosan and Au NPs/chitosan with varying loading amounts were all carried out. The characteristic peak of N–H stretching vibration appeared at 3300–3500 cm^{-1} in all samples. Base on previous reports, the gradual blue shift of transmittance in this band region with increasing metal loading amounts should be observed due to the interaction of N–H and metal ions or nanoparticles.[51] However, this change was negligible in present system, which might be due to the possibility of overlapping between N–H and O–H stretching vibrations. Fortunately, it is worth noting that the formation of Au NPs/chitosan generates two new bands at about 1735 and 1750 cm^{-1}, which is ascribed to the carbonyl stretch vibrations in aldehydes, ketones and carboxylic acids. These new peaks in the composites imply that the redox reaction includes the reduction of $AuCl_4^-$ and oxidation of the hydroxyl groups in the chitosan skeletons. Present assumption is consistent with previous work reported by Panigrahi et al. and Wei et al.[51, 52]

With these Au NPs/chitosan composites in hand, we tend to evaluate their performance in catalysis. The reduction of 4–nitrophenol (4–NP) by excessive $NaBH_4$ as a model reaction is selected to test the catalytic activity of Au NPs/chitosan. Generally, the reaction was carried out under ambient

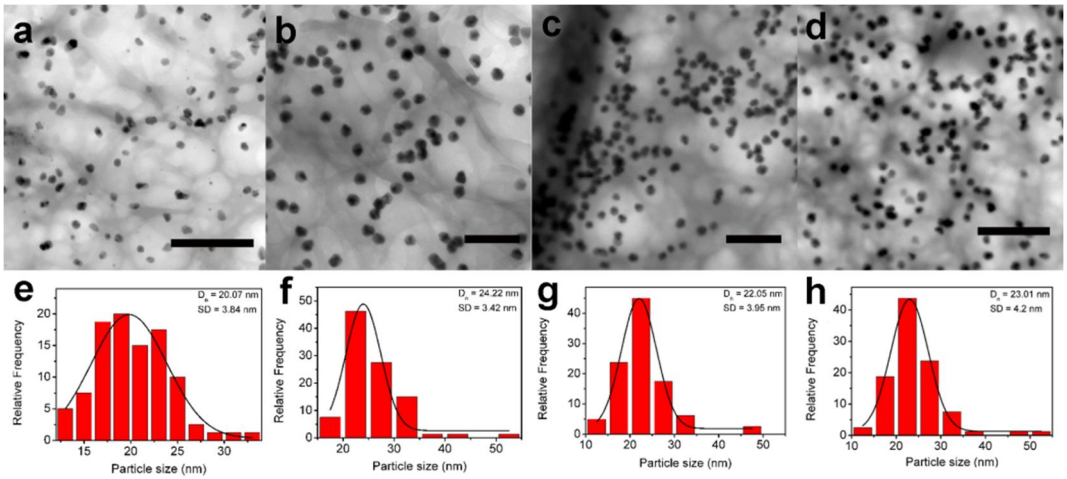

Fig. 2 TEM images of Au NPs/chitosan as a function of various Au loading amounts from a) 0.3125 wt%, b) 0.625 wt%, c) 1.25 wt%, and d) 2.5 wt%. e), f), g), and h) are corresponding particle sizes distributions. The average sizes and standard deviation are listed in the right corners. Particle sizes are ranging from 20 to 24 nm, which is consistent with the UV–vis results. The scale bar is 100 nm.

conditions. The 4–NP solution shows a strong absorption peak at 317 nm in neutral or acidic conditions. Upon the addition of $NaBH_4$ solution, the position of characteristic peak of 4–NP shifted from 317 to 400 nm immediately because of the formation of 4–nitrophenolate ion, accompanying the color change of light yellow to yellow–green. Despite $NaBH_4$ is regarded as a strong reducing agent, it is inert for the reduction of 4–NP in the absence of Au NPs/chitosan, as confirmed by the unaltered absorption peak at 400 nm for a long duration in **Fig S1a** in supporting information and **Fig. 4b**. Interestingly, after the addition of Au NPs/chitosan with 0.625% Au loading amount, the color of the 4–nitrophenolate ions was invisible after 150 s, as shown in inset of **Fig. 4a**. The decoloration process was recorded by UV–vis spectroscopy. As shown in **Fig. 4a**, the characteristic absorption peak of 4–nitrophenolate ion at 400 nm gradually decreased, while new peak of 4–AP appeared at 295 nm. In the cases of other Au loading amounts catalysts, the reduction reactions complete in 67 to 840 s under similar conditions. In order to check out the catalytic nature of catalyst, the reduction reaction of 4–NP only in the presence of chitosan was performed. It is obvious to see in **Fig. S1b** in supporting information and **Fig. 4b** that the 4–NP characteristic peak intensity at 400 nm was unchanged even after 800 s incubation.

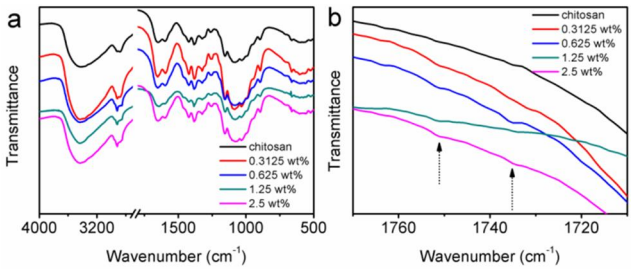

Fig. 3 FTIR spectra of a) chitosan and b) Au NPs/chitosan vibrations enlarged in the wavenumber range from 1710 to 1770 cm^{-1}. Black arrow indicated the newly emerged peaks after loading Au nanoparticles.

In order to get apparent kinetic rate constants K_{app}, $\ln(C_t/C_0)$ and C_t/C_0 versus reaction time for the reduction of 4–NP over different Au loading amounts catalysts were plotted in **Fig. 4b**. The kinetic constants K_{app} were 3.51×10^{-3}, 2.15×10^{-2}, 5.61×10^{-2}, and 2.59×10^{-2} s^{-1} corresponding to 0.3125 wt%, 0.625 wt%, 1.25 wt% and 2.5 wt% Au loading amounts in chitosan, respectively. It is evident that Au NPs/chitosan with 1.25 wt% loading exhibits the highest K_{app} among all the checked samples. Meanwhile, the turn–over frequency of all samples from low to high Au NPs loading amounts are 0.076, 0.21, 0.24 and 0.055 $mmol \cdot g^{-1} \cdot s^{-1}$, respectively. It is found that the catalytic efficiency increased gradually with increasing Au NPs loading amounts below 1.25 wt%. However, 2.5 wt% Au NPs loading amount sample resulted in the decreased catalytic efficiency. To our knowledge, the Au NPs supported on the nanocarrier can function as the electron mediator between 4–AP (oxidant) and BH_4^- (reductant), and the electron transfer happens via the Au nanoparticles.[47, 53, 54] It has been confirmed that the rate of electron transfer at the Au NPs surface was affected by the diffusion of 4–NP to the metal surface, interfacial electron transfer, and the diffusion of generated 4–AP away from the Au NPs surface.[55] Furthermore, the small sized Au NPs in present system, which possessed a higher redox potential value, are beneficial for accelerating the heterogeneous electron transfer. Meanwhile, Chen et al. and Esumi et al. both proved that the reduction of 4–NP in the presence of $NaBH_4$ by Au NPs/polymer was diffusion–controlled.[47, 55, 59] In addition, this diffusion–controlled mechanism can be ascribed to the chitosan matrix, in which Au NPs were synthesized and stabilized. Therefore, too much higher Au loading will result in the embedment inside the chitosan matrix, viz., the mass transfer of 4–NP into the inside of chitosan to approach the catalytic sites will be blocked. This is also proved by the fact that the K_{app} constants of Au NPs/chitosan with 1.25 wt% were higher than other loading amounts, and also much higher than other reported substrate–supported Au catalysts.[56–65]

From practical point of view, the recovery of Au NPs/chitosan is the burning issue, otherwise that will result in the high cost and environmental contaminations due to the residual metal species. Hence, we tend to embed magnetic species into the

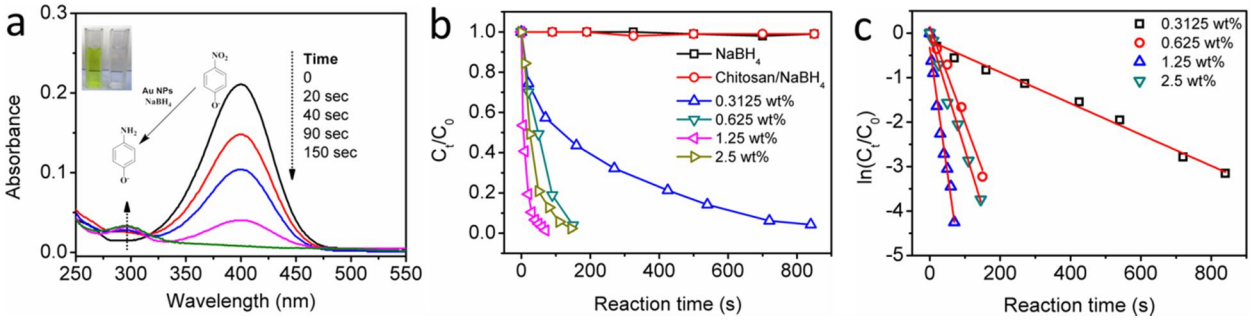

Fig. 4 (a) UV–vis absorption spectra during the catalytic reduction of 4–NP over Au NPs/chitosan with 0.626 wt% loading nanocomposite. Inset is the digital image of solution before and after reduction; (b) C_t/C_0 and (c) $\ln(C_t/C_0)$ versus reaction time for the reduction of 4–NP over chitosan/Au with varying loading amounts, respectively. C_0 and C_t were the absorption peaks at 400 nm initially and at reaction time t.

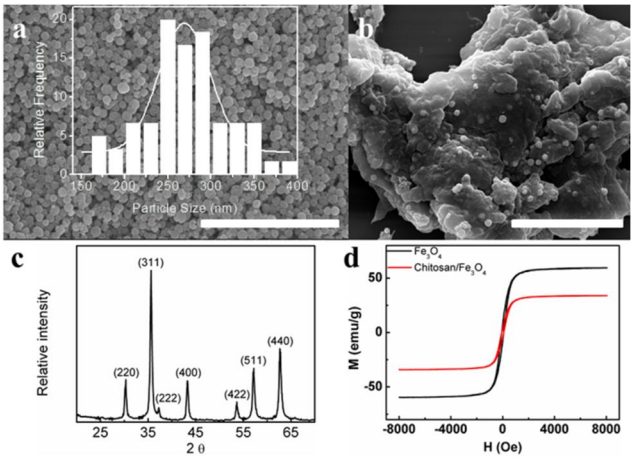

Fig. 5 (a) SEM image of Fe_3O_4 nanospheres, and inset is the size distribution; (b) SEM image of chitosan/Fe_3O_4 composite; (c) XRD of Fe_3O_4 nanospheres; (d) Room temperature hysteresis curves of the as–synthesized Fe_3O_4 with diameters of ca. 260 nm (black line), and chitosan/Fe_3O_4 composite (red line). The scale bar is 5 μm.

catalytic matrix. As is known to us, the magnetic separation technique possesses the advantages of rapidity, high efficiency, and cost–effectiveness. As shown in **Fig. 5a**, Fe_3O_4 nanospheres were fabricated according to a reported glycol–mediated method.[49] Inset of **Fig. 5a** illustrates the mean size of spheres is about 260 nm. Fe_3O_4 nanospheres were dispersed into chitosan aqueous solution including 0.05 M acetic acid. The Fe_3O_4/chitosan composite was precipitated by the addition of 1 M NaOH aqueous solution. The strong complexation ability of chitosan with Fe_3O_4 originated from the sharing of lone electron pairs from the nitrogen atom in amine with Fe^{II} or Fe^{III}. This is to say, the strong interactions between these two components guarantee the stability during the following reactions. As confirmed in **Fig. 5b**, Fe_3O_4 nanospheres were distributed evenly in the chitosan matrix. Additionally, the diffraction patterns and relative intensities of all peaks in XRD results shown in **Fig. 5c**, accord with those of magnetite (Joint Committee on Powder Diffraction Standards (JCPDS) File Card No. 19–0629). The magnetization curves, as shown in **Fig. 5d**, display the saturation magnetizations of Fe_3O_4 and chitosan/Fe_3O_4 composite. The saturation magnetization of Fe_3O_4 decreased from 59 emμ/g to 34 emμ/g after embedding in chitosan at 20 wt% loading amounts, which enables instantaneous magnetic separation.[66]

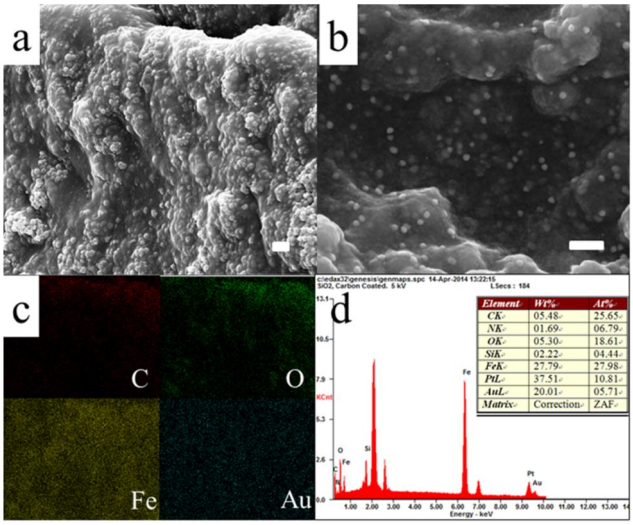

Fig. 6 Low (a) and high (b) magnification SEM images of Au NPs/chitosan/Fe_3O_4 composite, respectively; (c) EDS mapping images of C, O, Fe and Au elements in image a; (d) EDS spectra and atomic ratio of corresponding elements in Au NPs/chitosan/Fe_3O_4 composite. The scale bars are 1 μm in (a), and 100 nm in (b).

The Au loading method on chitosan/Fe_3O_4 was similar to that of pure chitosan. As shown in **Fig. 6a**, Fe_3O_4 nanospheres were evenly embedded in the chitosan matrix, which is in accordance with the results of chitosan/Fe_3O_4 before Au NPs loading. The mild Au NPs loading condition is friendly to maintain the structure of magnetic composite. Meanwhile, the high magnification SEM image in **Fig. 6b** clearly illustrated the Au NPs on the surface of composite. Mapping and spectrum of energy–dispersive spectroscopy (EDS) in **Fig. 6c** and **6d** further confirmed the successful synthesis of Au NPs. Base on the survey of catalytic performance of Au contents, Au NPs/chitosan/Fe_3O_4 composite with 1.25 wt% Au loading amount is selected as a model system to evaluate the catalytic performance of the reduction of 4–NP. Similar to the reaction conditions of Au NPs/chitosan composite, the characteristic absorption peak of 4–nitrophenolate ion at 400 nm gradually

decreased, while new peak of 4–AP appeared at 295 nm after addition of Au NPs/chitosan/Fe_3O_4 composites**.** The colour of the 4–nitrophenolate ions was quickly invisible in 90 s. Meanwhile, the apparent kinetic rate constant K_{app}, $\ln(C_t/C_0)$ and C_t/C_0 versus reaction time for the reduction of 4–NP over Au NPs/chitosan/Fe_3O_4 composites were plotted in **Fig. 7**. The kinetic constants K_{app} were 4.71×10^{-2} s^{-1}, which is only slight lower than that of Au NPs/chitosan with 1.25 wt% loading amount. Further, the rate constant is also larger than those reported in recent catalytic systems, as compared in **Table 1**.[56-65] Concomitantly, the catalyst could be easily recovered by the application of an external magnetic field. The introduction of Fe_3O_4 into chitosan endows the system magnetic recovery ability, while not hinder the catalytic performance towards the reduction of 4–NP.

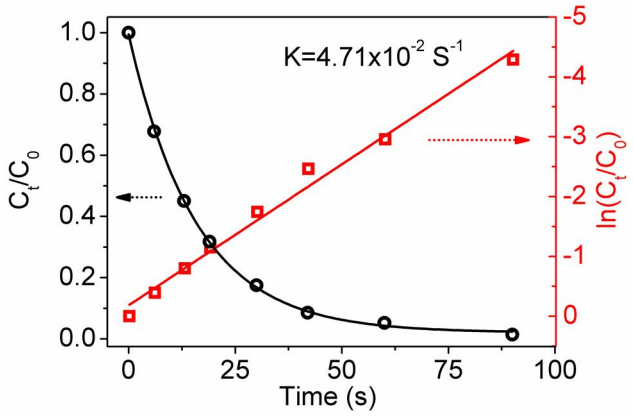

Fig. 7 The circles and squares were the $C_t C_0$ and (c) $\ln(C_t/C_0)$ versus reaction time for the reduction of 4–NP over Au NPs/chitosan/Fe_3O_4 composites with 1.25 wt% loading amounts. C_0 and C_t were the absorption peaks at 400 nm initially and at reaction time t.

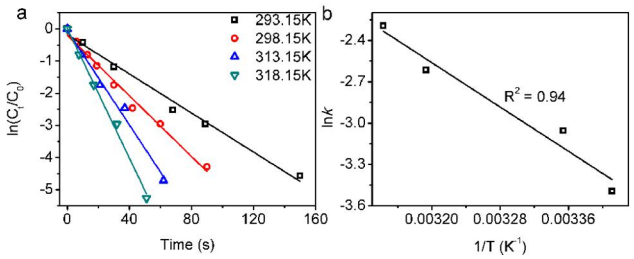

Fig. 8 Effect of reaction temperature on the rate constants of Au NPs/chitosan/Fe_3O_4 composites (a). Arrehenius plots of ln$k$ vs. 1/T for the reduction of 4–NP at 293.15, 298.15, 313.15, 318.15K (b). Temperature is controlled in oil bath.

The temperature dependent kinetic studies for the reduction of 4–NP was also evaluated. As shown in **Fig. 8a**, the rate constants at different temperatures were calculated from the slope of each plot of $\ln(C_t/C_0)$ vs. time. It was found that the catalytic performance of Au NPs/chitosan/Fe_3O_4 composite enhanced with increasing reaction temperatures. As has been known, activation energy (E_a), as an empirical parameter for all chemical reactions, could reflect the temperature dependency of the rate constants.[67] Arrhenius theory was generally applied to obtain the E_a from the relationship between rate constant and reaction temperature. The Arrhenius equation is depicted as follows:

$$\ln k = \ln A - \frac{E_a}{RT} \qquad (1)$$

where k is the first–order rate constant, A is the Arrhenius factor, E_a is activation energy, R is the universal gas constant, and T is the reaction temperature (in Kelvin). The catalytic reduction of 4–NP was carried out at 293.15, 298.15, 313.15, 318.15K. Based on the analysis of linear fitting of ln$k$ vs. 1/T in **Fig. 8b**, the activation energy was 33.4 kJ/mol calculated from the slope. This value is varied from those in previous works, which might be ascribed to the different chemical environment and reducing methods of Au NPs.[68] E_a of our catalyst is relatively large illustrates that the rate constant k is dependent on reaction temperature in present catalytic system.

Table 1 Comparison of kinetic constant (k_{app}) for the reduction of 4–NP in recent catalytic systems.

Entry	Catalyst	k_{app} (s^{-1})	Ref.
1	AuNPs@CSNFs	5.9×10^{-3}	57
2	Pd–Fe_3O_4@SiO_2	2.01×10^{-2}	61
3	Ag–M45	5.23×10^{-3}	62
4	Au–Fe_3O_4	2.93×10^{-2}	63
5	AuNPs–NSHNFs	1.2×10^{-2}	64
6	Ag@Me_{10}CB[5]	1.31×10^{-3}	65
7	Ag/MFC	1.71×10^{-2}	68
8	Au NPs/chitosan	5.61×10^{-2}	This work
9	Au NPs/chitosan/Fe_3O_4	4.71×10^{-2}	This work

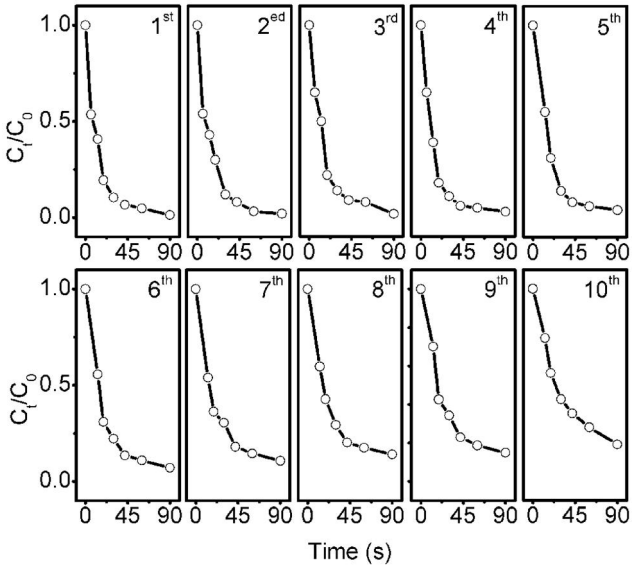

Fig. 9 Ten consecutive cycling reduction curves of 4–NP over Au NPs/chitosan/Fe_3O_4 composites in the presence of $NaBH_4$. The catalysts were recycled by applied magnetic field, and washed by distilled water for three times.

Generally, filtration or centrifugation methods are employed to recover the catalysts without the magnetic separation feature. The great loss of catalytic species will gradually decrease the catalytic efficiency. It is worth noting that magnetic separation based on Fe_3O_4 has perfect recovery efficiency and facile maneuverability. As shown in **Fig. 9**, the catalysts were recycled by applied magnetic field, and washed by distilled water for three times, subsequently subjected to the next

reaction without any drying treatment. The conversion of 4–NP to 4–AP was 81% in 90 s after 10th cycles. The reusable activity of Au NPs/chitosan composites at 90 °C was found to be extremely poor in the second cycle in previous work, which ascribed to the poison of active sites in Au NPs surface by the absorption of reactant or product. However, based on most previous works about the reduction of 4–NP by Au NPs, the catalytic efficiency can be retained well during the following reuse.[14, 35, 47, 59] The deactivation of catalytic efficiency of Au NPs are generally assigned to the agglomeration of nanosized particles causing the shrink of specific surface area, or the loss of total amounts of Au NPs on the supports. It is assumed that the unexpected results in the case of Au NPs prepared at 90 °C might be attributed to the catalyst preparing conditions or, viz., the intrinsic properties including the electronic properties or activating ability of Au NPs towards inert reagents will be greatly affected by the size, morphology, chemical environment, etc.[51] Hence, further study are required to fully evaluate the performance of Au NPs on chitosan prepared by varying method, and disclose the underlined mechanism by the assistance of theoretical simulation strategy.

Conclusions

A facile method was developed to prepare magnetically recoverable Au NPs/chitosan/Fe_3O_4 composites by the integration of biopolymer supports, catalytic centers and magnetic species. Au NPs were prepared at mild condition (50 °C) in the presence of chitosan as reducing and stabilizing agents, simultaneously chitosan was functioned as NPs supports. The as–prepared composites exhibited intriguing performance towards the reduction of 4–nitrophenol in the presence of $NaBH_4$. The decoloration process was recorded by UV–vis spectra, and the catalytic kinetics was also analyzed. It was found that the catalytic performance of Au NPs/chitosan/Fe_3O_4 remained 81% over tenth recycles. The superior advantages of present systems are three folds as follows. (1) The catalyst can be easily recovered by the application of an external magnetic field. (2) The ecofriendly synthetic procedure is in accordance to stringent requirement of green chemistry. (3) Apart from the application in the reduction of 4–NP, the biocompatibility and biodegradability of present Au NPs/chitosan/Fe_3O_4 promote the potential applications in biochemical related catalysis or therapy. Thus, present work might open a new avenue for the preparation of other types of metal NPs and chitosan composites taking the advantages of natural polymers, and provide a clue for facile incorporating magnetic centers into the integrated systems.

Acknowledgements

Financial supports from the Fundamental Research Funds for the Central Universities (Grant No. HIT. NSRIF. 2011025), SKLUWRE of HIT (QA201022), China Postdoctoral Science Foundation Funded Project (No. 20100471060, 2012T50313), and Natural Science Foundations of China (Nos. 21103035).

Notes and references

[a] State Key Lab of Urban Water Resource and Environment & Key Lab of Microsystem and Microstructure of the Ministry of Education, Harbin Institute of Technology, Harbin, Heilongjiang 150080, China. E–mail: hupa@hit.edu.cn

[b] School of Life Science and Technology, Harbin Institute of Technology, 92 West Dazhi Street, Harbin, Heilongjiang, 150001, P.R. China.

† Electronic Supplementary Information (ESI) available: [control experiments in the absence of Au NPs and UV–vis spectra measurements]. See DOI: 10.1039/b000000x/

1. T. Pradeep, *Thin Solid Films*, 2009, **517**, 6441.
2. T. K. Sau, A. L. Rogach, F. Jäckel, T. A. Klar and J. Feldmann, *Adv. Mater.*, 2010, **22**, 1805.
3. R. R. Arvizo, S. Bhattacharyya, R. A. Kudgus, K. Giri, R. Bhattacharya and P. Mukherjee, *Chem. Soc. Rev.*, 2012, **41**, 2943.
4. G. V. Hartland, *Chem. Rev.*, 2011, **111**, 3858.
5. S. Eustis and M. A. El–Sayed, *Chem. Soc. Rev.*, 2006, **35**, 209.
6. M.–C. Daniel and D. Astruc, *Chem. Rev.*, 2004, **104**, 293.
7. E. E. Connor, J. Mwamuka, A. Gole, C. J. Murphy and M. D. Wyatt, *Small*, 2005, **1**, 325.
8. G. Shore, W. J. Yoo, C. J. Li and M. G. Organ, *Chem.–Eur. J.*, 2010, **16**, 126.
9. Y. Sun and Y. Xia, *Science*, 2002, **298**, 2176.
10. J. Chen, F. Saeki, B. J. Wiley, H. Cang, M. J. Cobb, Z.–Y. Li, L. Au, H. Zhang, M. B. Kimmey and X. Li, *Nano Lett.*, 2005, **5**, 473.
11. Y. Wang, K. C. Black, H. Luehmann, W. Li, Y. Zhang, X. Cai, D. Wan, S.–Y. Liu, M. Li and P. Kim, *ACS Nano*, 2013, **7**, 2068.
12. Y. Wang, Y. Liu, H. Luehmann, X. Xia, D. Wan, C. Cutler and Y. Xia, *Nano Lett.*, 2013, **13**, 581.
13. T. Zeng, X. Zhang, S. Wang, Y. Ma, H. Niu and Y. Cai, *J. Mater. Chem. A*, 2013, **1**, 11641.
14. J. Zhang, G. Chen, M. Chaker, F. Rosei and D. Ma, *Appl. Catal. B*, 2013, **132**, 107.
15. Y. Min, M. Akbulut, K. Kristiansen, Y. Golan and J. Israelachvili, *Nat. Mater.*, 2008, **7**, 527.
16. T. Atay, J.–H. Song and A. V. Nurmikko, *Nano Lett.*, 2004, **4**, 1627.
17. N. R. Jana, L. Gearheart and C. J. Murphy, *Adv. Mater.*, 2001, **13**, 1389.
18. R. Lévy, N. T. Thanh, R. C. Doty, I. Hussain, R. J. Nichols, D. J. Schiffrin, M. Brust and D. G. Fernig, *J. Am. Chem. Soc.*, 2004, **126**, 10076.
19. T. Mironava, M. Hadjiargyrou, M. Simon, V. Jurukovski and M. H. Rafailovich, *Nanotoxicology*, 2010, **4**, 120.
20. E. Boisselier and D. Astruc, *Chem. Soc. Rev.*, 2009, **38**, 1759.
21. J. M. Balbus, A. D. Maynard, V. L. Colvin, V. Castranova, G. P. Daston, R. A. Denison, K. L. Dreher, P. L. Goering, A. M. Goldberg and K. M. Kulinowski, *Environ. Health Perspect.*, 2007, **115**, 1654.
22. A. Seaton, L. Tran, R. Aitken and K. Donaldson, *J. Royal Soc. Interface*, 2010, **7**, S119.
23. I. N. Remediakis, N. Lopez and J. K. Nørskov, *Angew. Chem. Int. Ed.*, 2005, **44**, 1824.
24. T. F. Jaramillo, S.–H. Baeck, B. R. Cuenya and E. W. McFarland, *J. Am. Chem. Soc.*, 2003, **125**, 7148.
25. M. Haruta and M. Daté, *Appl. Catal., A*, 2001, **222**, 427.
26. Y. Wang, S. Van de Vyver, K. K. Sharma and Y. Román–Leshkov, *Green Chem.*, 2014, **16**, 719.
27. M. Alhumaimess, Z. Lin, Q. He, L. Lu, N. Dimitratos, N. F. Dummer, M. Conte, S. H. Taylor, J. K. Bartley and C. J. Kiely, *Chem.–Eur. J.*, 2014.
28. M. Stratakis and H. Garcia, *Chem. Rev.*, 2012, **112**, 4469.
29. S. S. Kim, Y. R. Kim, T. D. Chung and B. H. Sohn, *Adv. Funct. Mater.*, 2014.
30. K. Sneha, M. Sathishkumar, S. Y. Lee, M. A. Bae and Y.–S. Yun, *J. Nanosci. Nanotechnol.*, 2011, **11**, 1811.
31. M. K. Corbierre, N. S. Cameron, M. Sutton, S. G. Mochrie, L. B. Lurio, A. Rühm and R. B. Lennox, *J. Am. Chem. Soc.*, 2001, **123**, 10411.
32. B. Li and C. Y. Li, *J. Am. Chem. Soc.*, 2007, **129**, 12.
33. T. KumaráSarma, *Chem. Commun.*, 2002, 1048.
34. Y. Shin, I.–T. Bae, B. W. Arey and G. J. Exarhos, *J. Phys. Chem. C*, 2008, **112**, 4844.
35. C. Yuan, W. Luo, L. Zhong, H. Deng, J. Liu, Y. Xu and L. Dai, *Angew. Chem. Int. Ed.*, 2011, **50**, 3515.

36. M. N. Ravi Kumar, *React. Func. Polym*., 2000, **46**, 1.
37. M. Rinaudo, *Prog. Polym. Sci.*, 2006, **31**, 603.
38. L. Ilium, *Pharm. Res.*, 1998, **15**, 1326.
39. F.–N. Allouche, E. Guibal and N. Mameri, *Colloids Surf., A*, 2014.
40. D. Wei and W. Qian, *Colloids Surf., B*, 2008, **62**, 136.
41. H. Huang and X. Yang, *Biomacromolecules*, 2004, **5**, 2340.
42. M. J. Laudenslager, J. D. Schiffman and C. L. Schauer, *Biomacromolecules*, 2008, **9**, 2682.
43. C. Sun, R. Qu, H. Chen, C. Ji, C. Wang, Y. Sun and B. Wang, *Carbohydr. Res.*, 2008, **343**, 2595.
44. R. Abu–Reziq, H. Alper, D. Wang and M. L. Post, *J. Am. Chem. Soc.*, 2006, **128**, 5279.
45. R. L. Oliveira, P. K. Kiyohara and L. M. Rossi, *Green Chem.*, 2010, **12**, 144.
46. S. Laurent, D. Forge, M. Port, A. Roch, C. Robic, L. Vander Elst and R. N. Muller, *Chem. Rev.*, 2008, **108**, 2064.
47. Y.–C. Chang and D.–H. Chen, *J. Hazard. Mater.*, 2009, **165**, 664.
48. S. Xuan, Y.–X. J. Wang, J. C. Yu and K. Cham–Fai Leung, *Chem. Mater.*, 2009, **21**, 5079.
49. K. Zhou, Y. Zhu, X. Yang and C. Li, *New J. Chem.*, 2010, **34**, 2950.
50. W. Wan Ngah, C. Endud and R. Mayanar, *React. Func. Polym.*, 2002, **50**, 181.
51. D. Wei, Y. Ye, X. Jia, C. Yuan and W. Qian, *Carbohydr. Res.*, 2010, **345**, 74.
52. S. Panigrahi, S. Basu, S. Praharaj, S. Pande, S. Jana, A. Pal, S. K. Ghosh and T. Pal, *J. Phys. Chem. C*, 2007, **111**, 4596.
53. P. L. Freund and M. Spiro, *J. Phy. Chem*, 1985, **89**, 1074.
54. D. S. Miller, A. J. Bard, G. McLendon and J. Ferguson, *J. Am. Chem. Soc.*, 1981, **103**, 5336.
55. K. Esumi, R. Isono and T. Yoshimura, *Langmuir*, 2004, **20**, 237.
56. Z. Zhang, C. Shao, P. Zou, P. Zhang, M. Zhang, J. Mu, Z. Guo, X. Li, C. Wang and Y. Liu, *Chem. Commun.*, 2011, **47**, 3906.
57. H. Koga, E. Tokunaga, M. Hidaka, Y. Umemura, T. Saito, A. Isogai and T. Kitaoka, *Chem. Commun.*, 2010, **46**, 8567.
58. S. Tang, S. Vongehr and X. Meng, *J. Mater. Chem.*, 2010, **20**, 5436.
59. K. Hayakawa, T. Yoshimura and K. Esumi, *Langmuir*, 2003, **19**, 5517.
60. K. Kuroda, T. Ishida and M. Haruta, *J. Mol. Catal. A: Chem.*, 2009, **298**, 7.
61. M. An, J. Cui and L. Wang, *J. Phy. Chem. C*, 2014, **118**, 3062.
62. B. Duan, F. Liu, M. He and L. Zhang, *Green Chem.*, 2014, **16**, 2835.
63. Q. Gao, A. Zhao, H. Guo, X. Chen, Z. Gan, W. Tao, M. Zhang, R. Wu and Z. Li, *Dalton Trans.*, 2014, **43**, 7998.
64. R. Jin, Y. Yang, Y. Li, L. Fang, Y. Xing and S. Song, *Chem. Commun.*, 2014, **50**, 5447.
65. H.–F. Li, J. Lü, J.–X. Lin and R. Cao, *Inorg. Chem.*, 2014, **53**, 5692.
66. J. Du and C. Jing, *J. Phys. Chem. C*, 2011, **115**, 17829.
67. S. Saha, A. Pal, S. Kundu, S. Basu and T. Pal, *Langmuir*, 2009, **26**, 2885.
68. M. Zhu, C. Wang, D. Meng and G. Diao, *J. Mater. Chem. A*, 2013, **1**, 2118.

Table of contents

Environmentally benign magnetic Au NPs/chitosan/Fe_3O_4 composites: preparation and their catalytic reduction of 4–nitrophenol.